AD NUMBER
AD815777
LIMITATION CHANGES
TO: **Approved for public release; distribution is unlimited. Document partially illegible.**
FROM: **Distribution authorized to U.S. Gov't. agencies and their contractors; Critical Technology; JUN 1967. Other requests shall be referred to Army Electronics Command, Fort Monmouth, NJ. This document contains export-controlled technical data.**
AUTHORITY
per dtic form 55

AD

AD 825777

TECHNICAL REPORT ECOM-01666-6

HIGH-POWER HYBRID MULTIPLE-BEAM KLYSTRON FOR PHASED ARRAYS

SIXTH QUARTERLY PROGRESS REPORT

By

G. M. Branch—W. Neugebauer—H. L. Thal—J. R. M. Vaughan

JUNE 1967

ECOM

UNITED STATES ARMY ELECTRONICS COMMAND · FORT MONMOUTH, N.J.

SPONSORED BY: ADVANCED RESEARCH PROJECTS AGENCY - PROJECT DEFENDER
ARPA ORDER NO. 345, AMENDMENT NO. 2

CONTRACT DA 28-043-AMC-01666(E)

GENERAL ELECTRIC COMPANY
Schenectady, N. Y.

NOTICES

Disclaimers

The findings in this report are not to be construed as an official Department of the Army position, unless so designated by other authorized documents.

The citation of trade names and names of manufacturers in this report is not to be construed as official Government indorsement or approval of commercial products or services referenced herein.

Disposition

Destroy this report when it is no longer needed. Do not return it to the originator.

TECHNICAL REPORT ECOM-01666-6 JUNE 1967

HIGH-POWER HYBRID MULTIPLE-BEAM KLYSTRON
FOR PHASED ARRAYS

SIXTH QUARTERLY PROGRESS REPORT

15 DECEMBER 1966 TO 15 MARCH 1967

Report No. 6

CONTRACT NO. DA 28-043 AMC-01666(E)

Prepared by

G. M. BRANCH — W. NEUGEBAUER — H. L. THAL -- J. R. M. VAUGHAN

GENERAL ELECTRIC COMPANY

SCHENECTADY, NEW YORK

For

U.S. ARMY ELECTRONICS COMMAND, Fort Monmouth, N. J.

Fort Monmouth, New Jersey

SPONSORED BY:

ADVANCED RESEARCH PROJECTS AGENCY

ARPA ORDER NO. 345, AMENDMENT NO. 2

DISTRIBUTION STATEMENT

This document is subject to special export controls and each transmittal to foreign governments or foreign nationals may be made only with prior approval of CG, USAECOM, ATTN: AMSEL-KL-TM, Fort Monmouth, New Jersey 07703

ABSTRACT

The purpose of this contract is the development of a high-power broadband amplifier using the principles of a traveling-wave multiple-beam klystron. The method being followed is to (a) design the beam and the interaction impedances by a computer study, (b) build a single-beam prototype for checking the calculations and obtaining final data, and (c) construct a full-power 15-beam tube.

At this point in the program, the beam and interaction designs have been completed, and fabrication of the single-beam prototype tube is almost complete. Test equipment for the single-beam tube has been set up; the modulator for the 15-beam tube has been designed, and major components are being received. The electromagnet for the 15-beam tube is in place, and the single-beam tube is to be tested in various positions in it.

Conclusions: All basic elements for the single-beam prototype have been designed, fabricated, and tested. The assembly is almost complete, and processing and testing of this tube can now proceed. No major problems are foreseen.

TABLE OF CONTENTS

LIST OF ILLUSTRATIONS

LIST OF TABLES

REPORT

A. STATEMENT OF PROBLEM

The objective of this program is to design and build a C-Band amplifier of high peak and average powers and broad bandwidth, using the principle of a multiple-beam klystron. The objective specification is included as Table I.

B. BACKGROUND AND APPROACH TO THE PROBLEM

Following earlier efforts to build traveling-wave multiple-beam klystrons in which the beam interactions intermediate between the input and output circuits were with traveling waves, it was determined that the required combination of bandwidth and efficiency could best be obtained by the use of traveling-wave input and output sections with standing-wave (cavity) intermediate interactions.

Based on these findings, the approach taken in the present work became:

(1) to compute a suitable set of interaction impedances for a single beam;

(2) to compute a gun design to supply this beam;

(3) to build beam testers as necessary to demonstrate the beam design;

(4) to build a single-beam RF tube to demonstrate the interaction design and obtain optimum impedance values; and

(5) to build a multiple-beam tube incorporating the results of these preliminary tests.

Items (1) and (2) are complete except for refinement as a result of further data. This report covers work on Items (3), (4), and (5), arranged in that order.

Table 1 - C-Band Hybrid [illegible] Objectives and Design Values

PARAMETER	[illegible]	[illegible]	UNITS
BEAM			
Pulse voltage	[illegible]	[illegible]	kV
Pulse current	[illegible]	[illegible]	A
Pulse power input	[illegible]	[illegible]	MW
Duty	[illegible]	[illegible]	
Pulse length, maximum	[illegible]	[illegible]	μSEC*
Average power input	[illegible]	[illegible]	kW
Perveance	[illegible]	[illegible]	μPERV
r_c	[illegible]		Cm
Cathode area	[illegible]		Cm^2
Cathode current density (peak)	[illegible]		A/Cm^2
Cathode current density (mean)	[illegible]		A/Cm^2
Area convergence ratio			
cathode area/tunnel area	[illegible]		
cathode area/beam area : approx.	[illegible]		
Depressed potential at exit	[illegible]		kV
Magnetic field (Brillouin)	[illegible]	[illegible]	Gauss
RF INPUT			
Center frequency	[illegible]		MHz
Lower band edge at -1 dB	[illegible]		MHz
Upper band edge at -1 dB	[illegible]		MHz
Drive power, peak, design value	[illegible]	[illegible]	W
maximum	[illegible]	[illegible]	W
RF OUTPUT			
Peak power		[illegible]	MW
Average power		[illegible]	kW
Efficiency	[illegible]**	[illegible]	%
Gain		[illegible]	dB
RF envelope rise time		[illegible]	nSEC
CAVITIES			
Tunnel diameter	[illegible]		inch
Gap length	[illegible]		inch
Drift length, buncher section	[illegible]		inch
Drift length, penultimate-to-output	[illegible]		inch
R/Q	[illegible]		
Gap coefficient (mid band), M	[illegible]		
Gap transit angle	[illegible]		
Normalized drift-tube radius, γa	[illegible]		
Normalized beam radius, γb	[illegible]		

* Both single-beam and [illegible]-beam tubes will be designed for [illegible]-μSEC operation, but only the single-beam tube can be tested at this pulse length.

**Not for build-up beams; [illegible]-beam value includes build-up beams.

C. RESULTS AND DISCUSSION OF RESULTS

Since, at this stage, the project involves several distinct lines of investigation and construction, progress in each area is reported and discussed in this section under the headings listed below:

1. Beam Tester
2. Power Dissipation in Loaded Cavities
3. Cavity and Waveguide Response Curves
4. Single Beam Tube Assembly
5. Test Equipment
6. Magnet
7. Impedance Taper for Output Waveguide

Beam Tester

Beam tester No. 6 was constructed with a tungsten cathode according to Computer Design Number 17. It was tested in a solenoid with cylindrical symmetry, and its performance at 60 kilovolts is given in Table II. Cathode emission was measured at a pulse length of 100 microseconds to verify the absence of any current droop. It was found that at

. . . .

Table II: Performance of Beam Tester No. 6

Peak Voltage	60.0 KV
Peak Current	18.6 A
Perveance	1.27 $\mu A/V^{3/2}$
Pulse Length	100 μSEC
Repetition Rate	30 PPS
Duty (Max. available from present test modulator)	0.003
Interception:	
Anode	0.03%
Body	0.44%
Collector Pole Piece (incl. secondaries)	0.88%
Collector	98.21%
Magnetic Field (Curve B)	2300 Gauss

no time, even when the cathode was operated temperature-limited, was there any observable change in perveance during the entire 100-microsecond pulse. Beam transmission through to the collector pole piece was better than 99 percent, with a magnetic field of 2550 gauss. At the design magnetic field of 1830 gauss, the transmission was 96.7 percent, with about 0.9 percent being intercepted at the collector pole piece in each case. The magnetic field profiles corresponding to these two cases are given in Figure 1. Both field values are within the design capability of the magnet being built for the 15-beam tube.

Figure 2 shows the cathode current as a function of voltage for various values of cathode temperature. The measured perveance of 1.27 is 2 percent below the design value of 1.3 microamperes volt$^{3/2}$. The cathode temperature must be 1030°C to avoid temperature-limited operation at 60 kilovolts.

The beam tester was X-rayed both cold and with the cathode at full temperature to verify the estimates of thermal expansion. It was found that the expansion of the entire cathode structure was 0.010 inch greater than had been estimated. The relative position of the cathode with respect to the focusing cup was also found to be off, but only by 0.003 inch. A new beam tester will be constructed with the correct hot dimensions and will be tested in both the cylindrical field and in the long rectangular field being made for the final 15-beam tube. Beam performance will be checked in various positions in the rectangular field to ensure acceptable operation of the multiple-beam tube.

Power Dissipation in Loaded Cavities

Using the computer data for design No. 86 (reported in Quarterly Progress Report No. 3), the power to be dissipated in each loaded cavity was calculated, and the results are plotted in Figure 3. In cavity 4 (the last double-tuned cavity) the peak power reaches 8000 watts at 5500 MHz, due to the sharp rise in I/I_0 at the low end of the band (see Figure 5 in Quarterly Progress Report No. 3), while in cavity 5 (the single-tuned loaded cavity) the peak value is 8500 watts at 5850 MHz, due in this case to the peaking of the cavity impedance (see Figure 4 in Quarterly Progress Report No. 3).

At the maximum duty of 0.01, these two cavities must therefore be capable of absorbing 80 to 100 watts average power without becoming overheated.

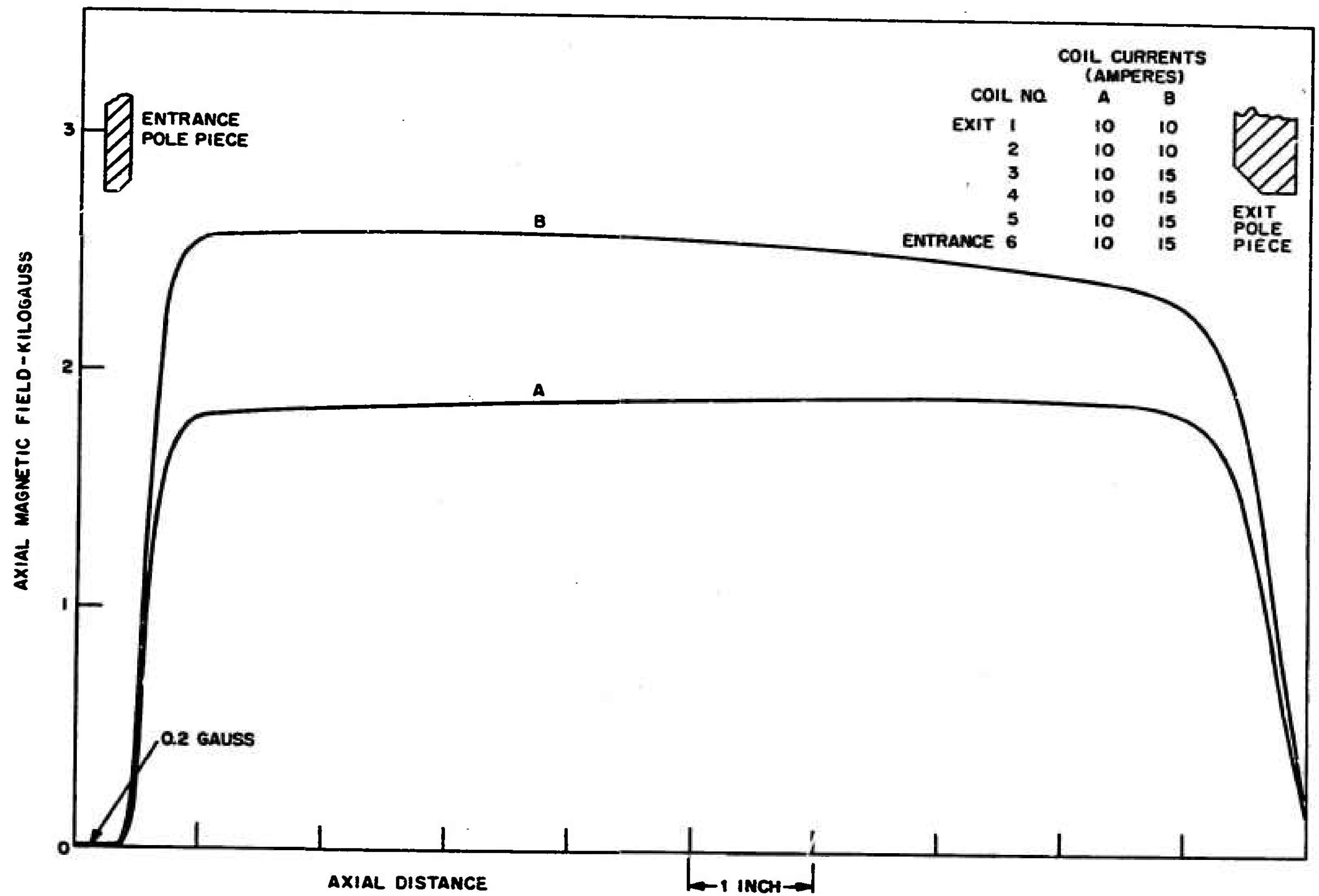

Figure 1 - Magnetic Field Profiles Along the Beam Axis

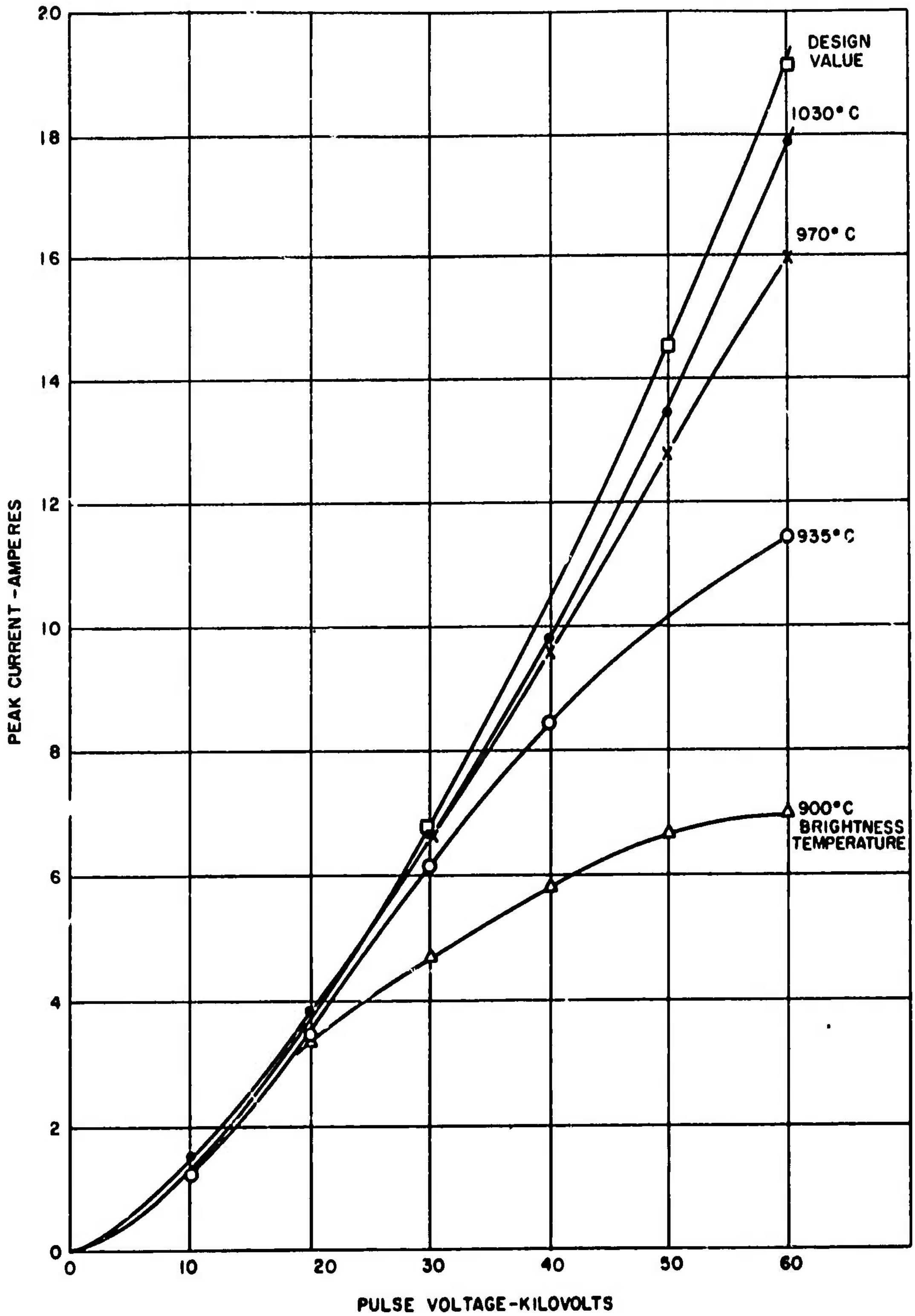

Figure 2 - Cathode Current Versus Pulse Voltage for Tungstate Cathode

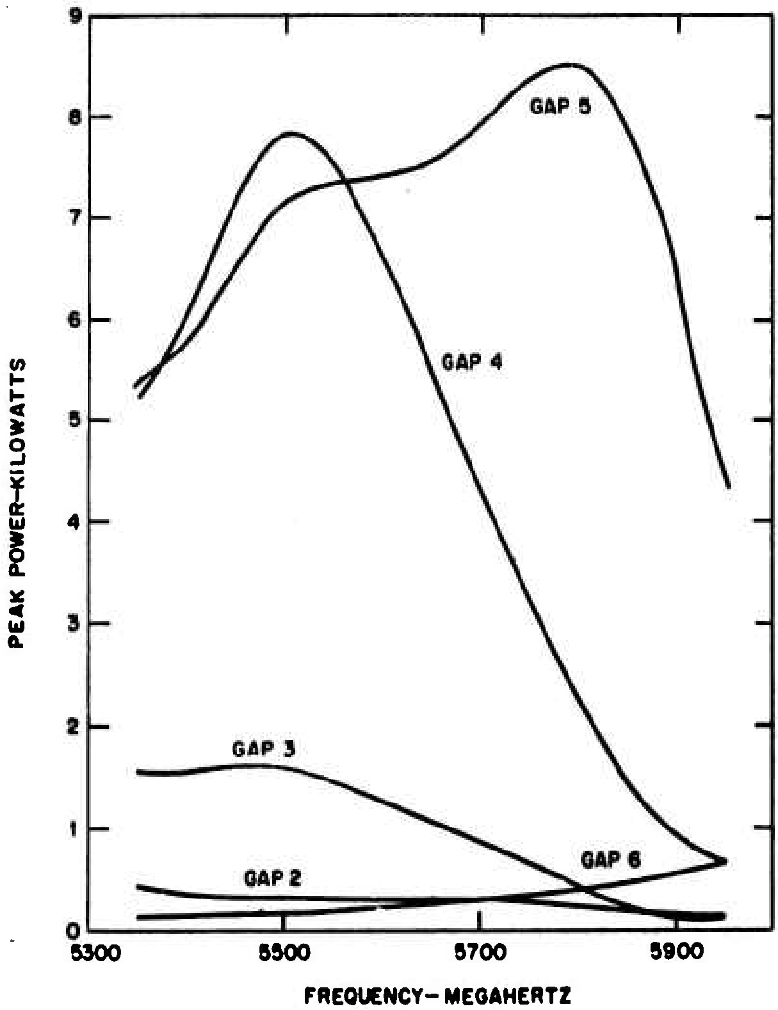

Figure 3 - Peak Power Absorption in Loaded Cavities
(Computer Design No. 86)

The heat conduction equation was solved for a rectangular block, cooled on the rear face, with energy entering by the front face and assumed to be absorbed in the material at a rate which decreases linearly to zero at the back face; this leads to the following equation for the steady-state temperature rise at the front surface:

$$T = \frac{2aW}{3AK} \qquad (1)$$

where: A is the cross-sectional area perpendicular to the heat flow (CM^2)

a is the depth parallel to the heat flow (CM)

K is the thermal conductivity (watts/CM^2/$^\circ$C/CM)

W is the power to be absorbed (watts), and

T is the temperature rise ($^\circ$C).

The greater precision of an exponential assumption about the absorption is not justified, because of considerable uncertainty in the value of K.

Using the book value of K[1], 0.04 watt/CM^2/$^\circ$C/CM, for the planned absorber arrangement in cavity 4, the calculated temperature rise was 960°C. While this was obviously excessive, it was still thought to be an underestimate, because the book value of K was probably applicable to compact SiC of near theoretical density, rather than the porous material being used.

To obtain directly relevant data, the specific heat and thermal conductivity of an actual specimen were measured. The values obtained were:

Specific heat:	0.25 calories/GM
Thermal conductivity K:	0.025 watt/CM^2/$^\circ$C/CM

This indicated that the average temperature rise would be even worse than first calculated, and that the absorber must be redesigned to decrease 'a' or increase 'A', or both, while still appearing as a good RF match.

1. Handbook of Thermophysical properties of Solid Materials, Goldsmith et-al. Vol. 3, VII-D.

Equation (1) is perhaps deceptively simple. With a fixed power W to be absorbed, reduction of the thickness 'a' raises the power density in the material at the same time it shortens the conduction path to the cooled wall. Intuition might suggest that the two effects would cancel out, but this is not so. The improved conduction outweighs the higher power density, so that the surface temperature becomes proportional to the thickness. One should therefore use the thinnest layer that is still capable of providing a good RF match.

After some trials, the arrangement of Figure 4 was adopted. Since the U-shaped molybdenum plate is installed in the cavity by means of a spring fit, cooling is obtained at the ends of both arms as well as at the center where the piece is fastened. The thickness 'a' is 0.25 CM, and the effective area 'A' is 9 CM^2. Inserting these values in equation (1), the expected temperature rise is approximately 60°C; if the cavity wall is held to 30°C, and the SiC surface should reach approximately 90°C.

A cavity with the absorber layout of Figure 4 was then tested at full average power by exciting it with a C-Band voltage tunable magnetron and a matched coupling loop, inserted through the beam tunnel. Stripes of temperature-sensitive paint were applied to the surface of the silicon carbide, and the power was raised to 80 watts. Color changes in the paint

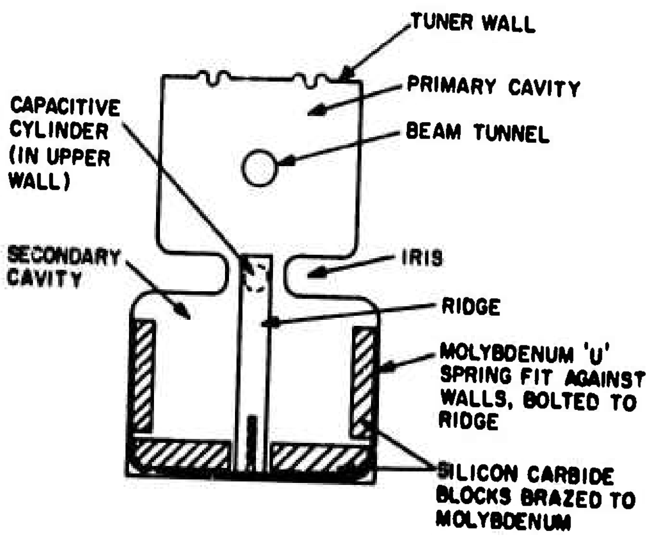

Figure 4 - Final Design of Loading for Cavities 2, 3, and 4

indicated temperatures between 95 and 145°C on the side walls, and under 95°C on the thicker blocks at the back. After operation at 120 watts -- 50 percent above the maximum in-service power level -- the 145°C color change occurred over the central area of each side piece, indicating a maximum temperature of probably 160 to 170°C. At this temperature, no outgassing problems are anticipated, after a 600°C bakeout.

The experiment indicated that this design is adequate for the average power that is expected; it also confirmed that the assumptions on which equation (1) is based are good enough for this kind of calculation, in which a precise result is not needed -- only an assurance that the working temperature will be well under the bakeout temperature.

Applying the same methods to the cavity 5 design, the calculated working temperature was under 200°C, and no change in this design was necessary.

The pulse temperature rise was also calculated; owing to the deep penetration of the power, and the relatively high specific heat (2-1/2 times that of copper), the pulse component was found to be completely negligible compared to the average temperature rise, for both cavities.

The dissipations in cavities 2 and 3 are, of course, small compared to that in cavity 4, so these pose no problem. The same loading is used, however, for the sake of uniformity.

Cavity and Waveguide Response Curves

When the revised cavity loading had been tested to the full average power, as described in the previous section, permanent loads were fitted to cavities 2, 3, 4, and 5. The response curves of these cavities are shown in Figure 5. The differences between these curves and those shown in Figure 4 of Quarterly Progress Report No. 3 are mainly due to the fact that the computed curves include the effect of beam loading, while the cold-test experimental curves do not. The responses obtained conform closely to the desired cold frequencies and Q values.

The response of cavity 6 is not shown, since without beam loading or internal loading, it is simply a spike at 6100 MHz. The frequency of the cavity, as brazed, was within 2 MHz of the design value.

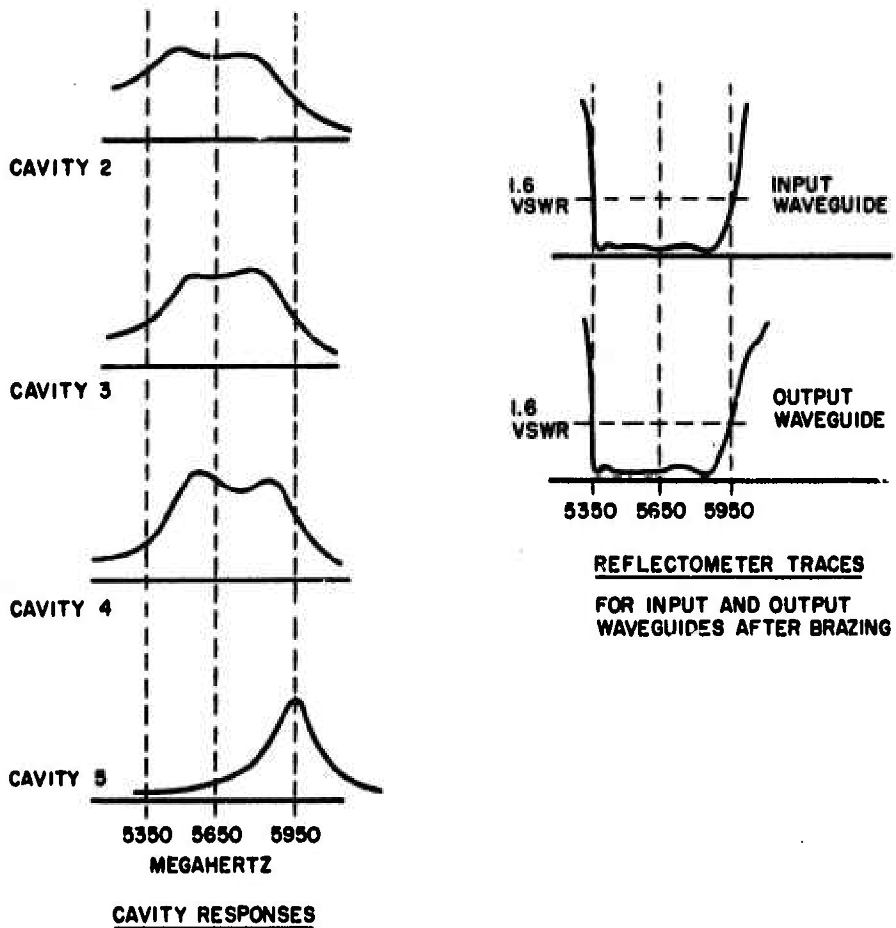

Figure 5 - Cavity Response Curves and Waveguide Reflectometer Curves (Traced from Oscilloscope Photos)

Also shown in Figure 5 are the reflectometer traces of the two waveguides, after brazing and final adjustment. The bandpass is shifted about 20 MHz downwards, compared to the brass cold-test models, probably due to small differences in the shapes of the fixed copper tunnel noses, compared to the earlier adjustable ones. The VSWR is a little high at the high frequency end of the band as a result, but is acceptable for the single-beam tube. The multiple-beam waveguide design is being adjusted to recenter the bandpass correctly.

Single-Beam Tube Assembly

Assembly of the single-beam tube has proceeded more slowly than expected. The major problem here has been distortion of the waveguides adjacent to the windows during brazing. Several windows were lost during attempts to rebraze; the alumina-ceramvar braze is adequately matched for many heat cycles up to 600°C, but rebrazing at 1000°C takes it well above the kink in the ceramvar expansion curve, and cracks have developed. The basic cause of the distortion appears to be the use of standard OFHC copper waveguide, which was perhaps a false economy. It is planned to redesign the windows for the 15-beam tube so that the ceramic braze is only subjected to one brazing cycle -- the next joint being a weld -- and to machine the waveguide sections from solid material.

At this time, the input and output waveguides and all the cavities have been brazed, aligned, and welded together. The cathode parts are all available, but are not being assembled to the tube until the window problems are solved, in order to protect the cathode surface. Four windows are on hand, but two of these are marginal, and completion of the tube is being delayed a few days while efforts are made to complete two fully satisfactory windows.

Figure 6 depicts the tube, with the body section welded, the external supporting structure in place, and the windows and cathode insulator clamped on.

Test Equipment

The test position for operating the single-beam tube, and providing the physical structure and magnetic field for the 15-beam tube, was completed. Measurements on the magnetic field are described in the next section (see "Magnet").

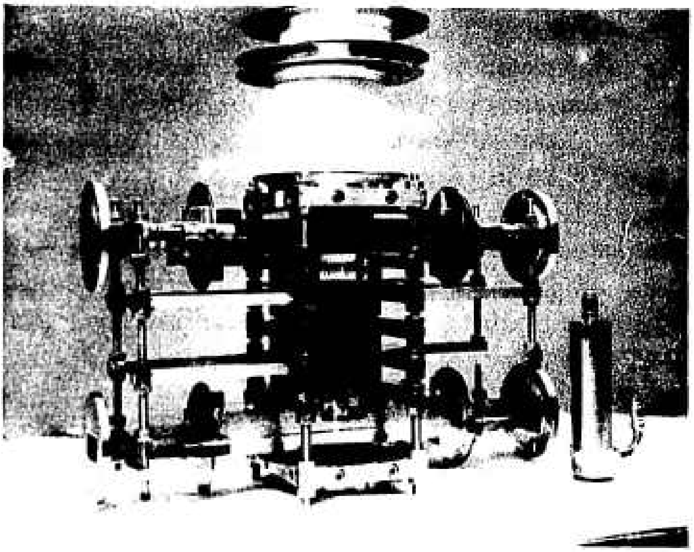

Figure 6 - Single-Beam Tube Showing Body Section, External Supporting Structure, Windows, and Cathode Insulator

The driver tube was received from IT&T, after a demonstration run in their plant. The gain of this tube is well over the specified minimum, with the result that a 100-mW output sweeping oscillator can be used as the primary RF source; the calibrated frequency sweep and the levelled output will be major convenience factors. The modulator for the driver tube has been installed and tested.

The 20 by 20 foot cage for the 15-MW, 150-KW modulator was completed; all major components are on order, and some have been delivered.

Magnet

The elongated magnet coils were received late in the reporting period. The winding irregularities were a little greater than expected, so that for the single-beam tube it has only been possible to stack 8 instead of the 9 coils that were planned; for the 15-beam tube, which will have no tuners, there is no restriction requiring that the gaps be lined up with the tuning screws, and for this tube it will be possible to use 9 (or even 10) coils.

However, the measured magnetic field, as a function of total coil current, is within 1 percent of the calculated value. Hence, the margins of safety that were allowed in designing the coils are not needed, and it will be possible to operate to over 2500 gauss with 8 coils while still remaining within the design maximum current for each coil. The intended range of operation is 1830 to 2500 gauss.

With plain pole-plates, the measured field dips 6.5 percent at the center of the magnet gap. The addition of 1/2 by 1/4-inch field straighteners along the outer edges of the pole-plates reduced the field variation across the gap to less than 2 percent, as shown in Figure 7.

End effects begin to be measurable when the beam holes are within 3.5 inches of the end of the pole-plate structure. Since the waveguide matching sections extend at least 3 inches from the end beams, the pole-piece extensions will contribute at most one inch to the length of the tube body.

Impedance Taper for Output Waveguide

The output filter circuit of a hybrid multiple-beam klystron consists of two regions -- a uniform-impedance build-up portion in which the voltage at each successive beam increases, and a power region in which the gap voltage at each beam is held essentially constant at its optimum value by reducing the circuit impedance at each beam to compensate for the additional power (see pages 1-3 of Quarterly Progress Report No. 1). Since the RF current induced in the output cavity of a klystron is a function of the RF voltage, each build-up beam will induce a different RF current into the output circuit. Figure 8 shows the computed relationship between current and voltage, plus a linear approximation which is suitable for voltages below the desired power-beam voltage.

Figure 9(a) is a schematic diagram of a build-up section having a uniform impedance Z_0. Only the forward-traveling current waves, I_f, will be considered in the design since backward waves induced by the beams will tend to cancel one another. Thus, since the forward-wave current is in-phase with the induced current, the forward currents entering and leaving the section will be related by:

$$I_{f(n+1)} = I_{f(n)} + \frac{1}{2} I_{n+1} \qquad (2)$$

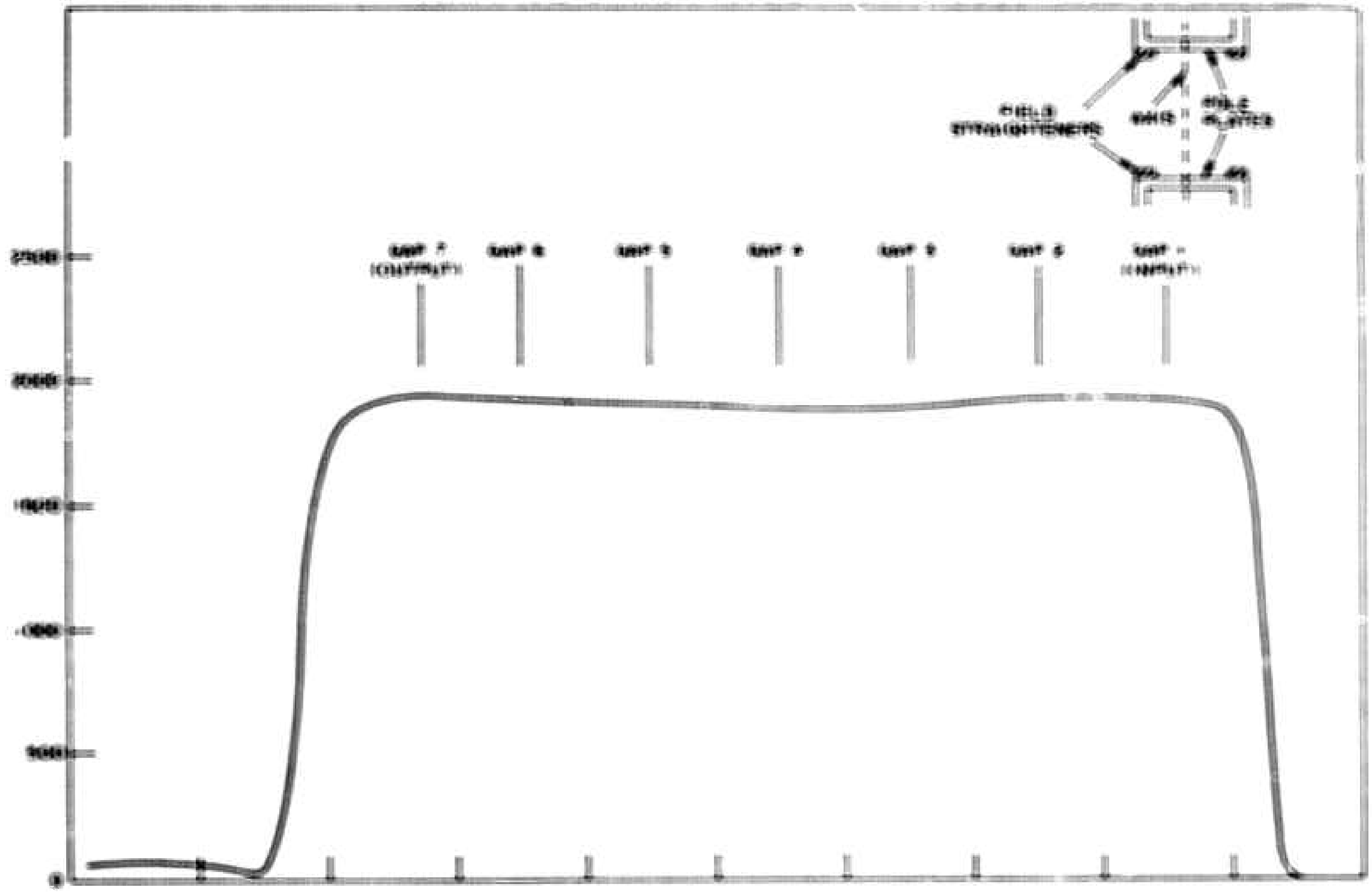

Figure 7 - Axial Field Plot with 1/2 + 1/4-inch Field Straighteners

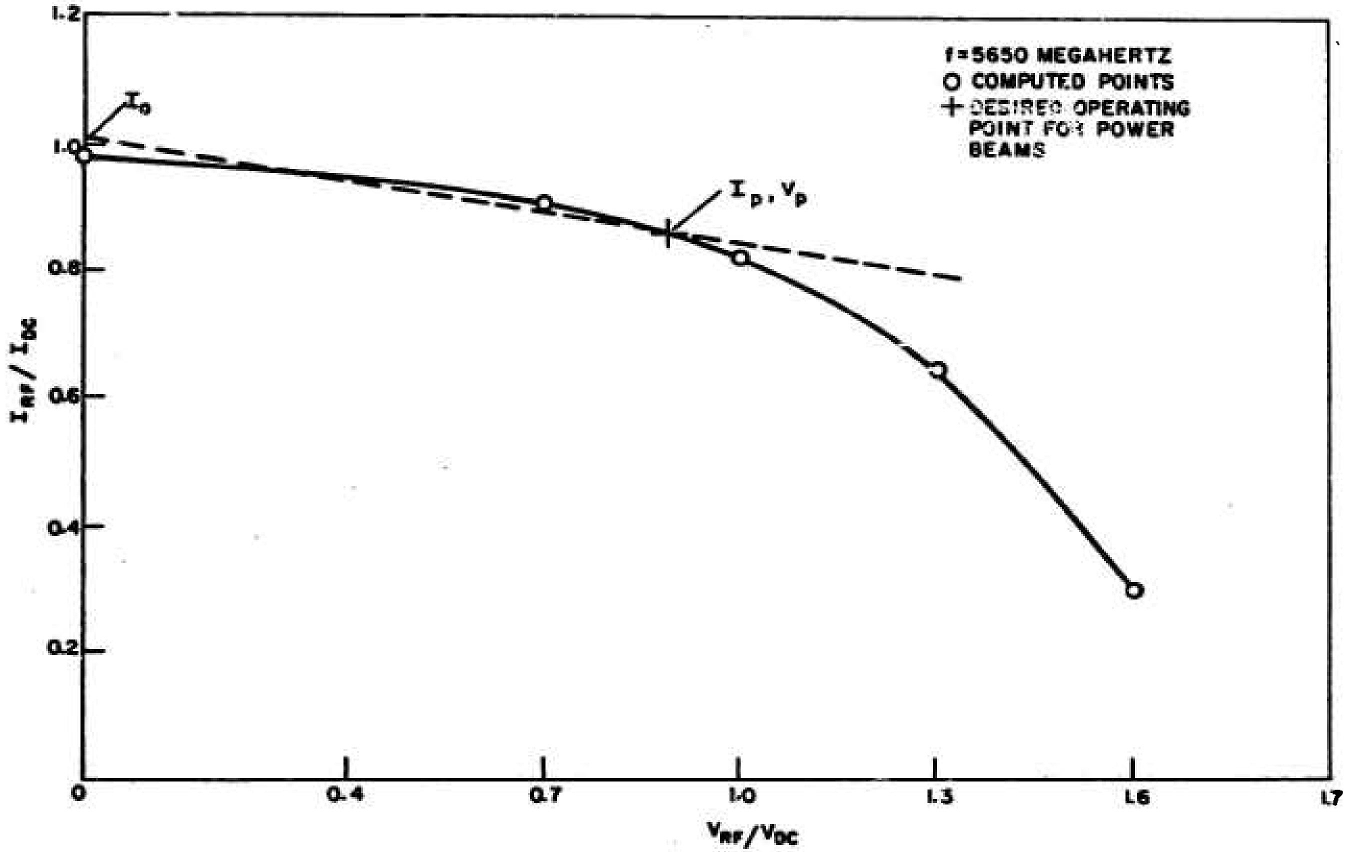

Figure 8 - Normalized RF Beam Current Versus Normalized RF Beam Voltage

(a)

(b)

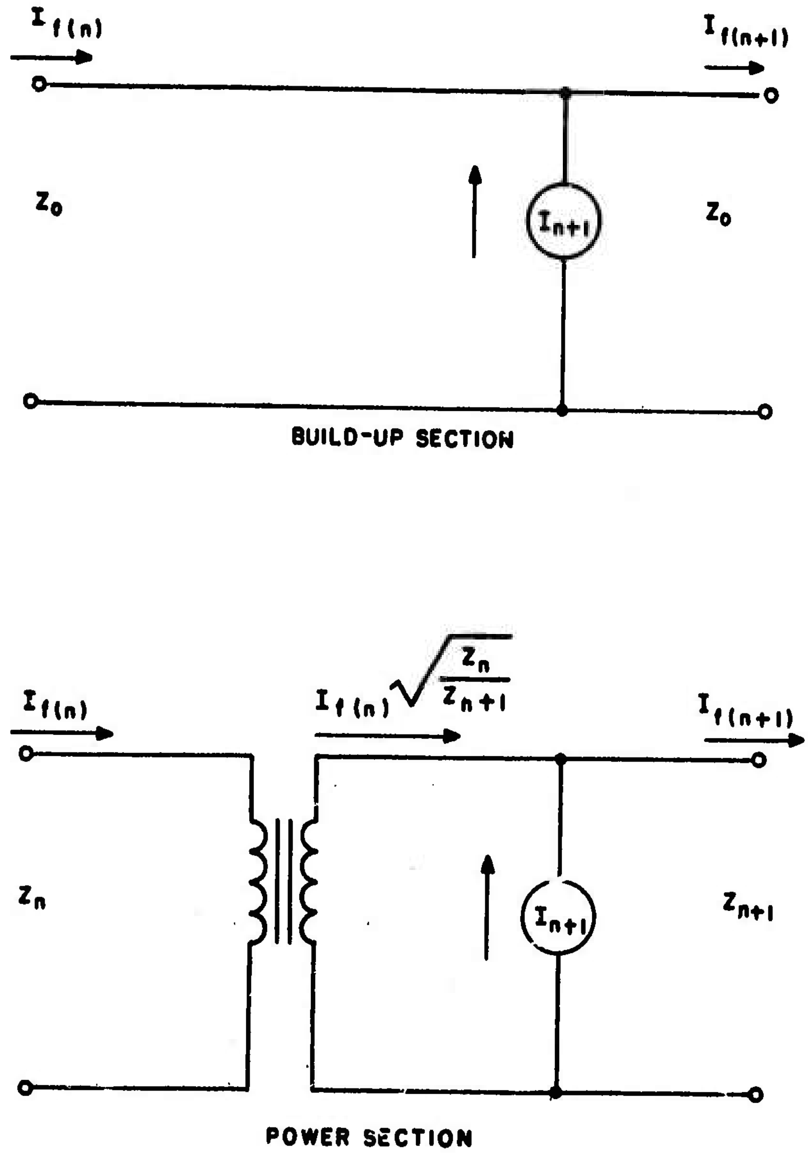

Figure 9 - Equivalent Circuits for Output Waveguide Sections

The induced current, I_{n+1}, may be related to the gap voltage by the following linear approximation:

$$I_{n+1} = I_o + \left[\frac{I_p - I_o}{V_p}\right] V_{n+1} \tag{3}$$

where I_p and V_p are the desired current and voltage of the power beams and I_o is the zero voltage intercept of the linear approximation as shown in Figure 8. Solving these equations for the voltage at the (n + 1) build-up beam yields:

$$V_{n+1} = \frac{Z_o \left[I_{f(n)} + \frac{1}{2} I_o\right]}{\left[1 - \frac{Z_o}{2}\left(\frac{I_p - I_o}{V_p}\right)\right]} \tag{4}$$

These recursion relations allow the voltage and current at each build-up beam to be calculated. When the equations yield a voltage exceeding V_p, that beam is in the power region instead of the build-up region, and its impedance must be reduced. Figure 9(b) depicts a power section in which the ideal transformer provides a matched transition between the impedances of adjacent sections. In this case:

$$I_{f(n+1)} = I_{f(n)} \sqrt{\frac{Z_n}{Z_{n+1}}} + \frac{1}{2} I_p \tag{5}$$

$$V_p = V_{n+1} = I_{f(n+1)} Z_{n+1} \tag{6}$$

Thus,

$$\frac{1}{2} I_p \left[\sqrt{Z_{n+1}}\right]^2 + I_{f(n)} \sqrt{Z_n} \left[\sqrt{Z_{n+1}}\right] - V_p = 0 \tag{7}$$

This quadratic equation can be solved to give Z_{n+1} in terms of Z_n and $I_{f(n+1)}$.

A BASIC computer program (THAL 21) for calculating the mid-band characteristic impedance for each section is given in Appendix A. A conservative preliminary taper design, based on ninety percent of the calculated current, is given in Table III. A final design can be computed after the current-voltage response of the single-beam prototype is measured.

Table III - Preliminary Taper Design

I_o = 17.46 Amps V_p = 53,550 Volts

I_p = 14.73 Amps Z_o = 2,260 Ohms

Beam Position	Circuit Impedance	Gap Voltage (KV)
1	2260	18.66
2	2260	36.30
3	2260	52.98
4	1470	53.55
5	1069	53.55
6	837	53.55
7	686	53.55
8	581	53.55
9	503	53.55
10	441	53.55
11	397	53.55
12	359	53.55
13	327	53.55
14	301	53.55
15	278	53.55

Low-Impedance Circuit

For the taper design given in Table III, the impedance must be reduced by a factor of 8.1. If the capacitively loaded waveguide used in the build-up section were scaled, the waveguide impedance would have to be reduced by a factor of 8.1, and the gap capacitance, increased in the same ratio. The resulting waveguide would be 0.062-inch high, with an interaction gap of the order of 0.020 inch. These close spacings would create mechanical problems and prohibitively high RF electric-field intensities, leading to field emission and arcing.

An alternate configuration for the low-impedance sections has been investigated. It consists simply of a uniform-width waveguide with two regions of different heights, as shown in Figure 10(a). This circuit matches the phase shift and impedance response of the capacitively loaded waveguide very closely, but has a gap (H2)* of 0.080 inch for the lowest impedance section.

The two-height filter can be accurately designed (neglecting the beam tunnel) without any experimental measurements. Since there are no variations in the transverse direction, the zero-mode cutoff of the filter occurs when the width is exactly one-half of a free-space wavelength, in the same manner as a uniform-height rectangular waveguide. The electric field pattern at this frequency, ω_o, is that obtained electrostatically by applying a voltage between the top and bottom faces (with the side walls removed).

The π-mode cutoff or resonance has short-circuit symmetry planes at the ends of the section shown in Figure 10(a). This π-mode cavity is equivalent to a portion of ridged-waveguide having a length equal to the filter width, W1. At the π-mode resonance, ω_π, W1 must equal one-half of the ridged-guide wavelength. Thus, the ridged-guide cutoff frequency, ω_r is given by:

$$\omega_r = \omega_\pi \sqrt{1 - \left(\frac{\omega_o}{\omega}\right)^2} \qquad (8)$$

---

*Variables occurring in the computer programs are written thus, rather than in subscript notation (H_2), to facilitate comparison of the equations with the programs.

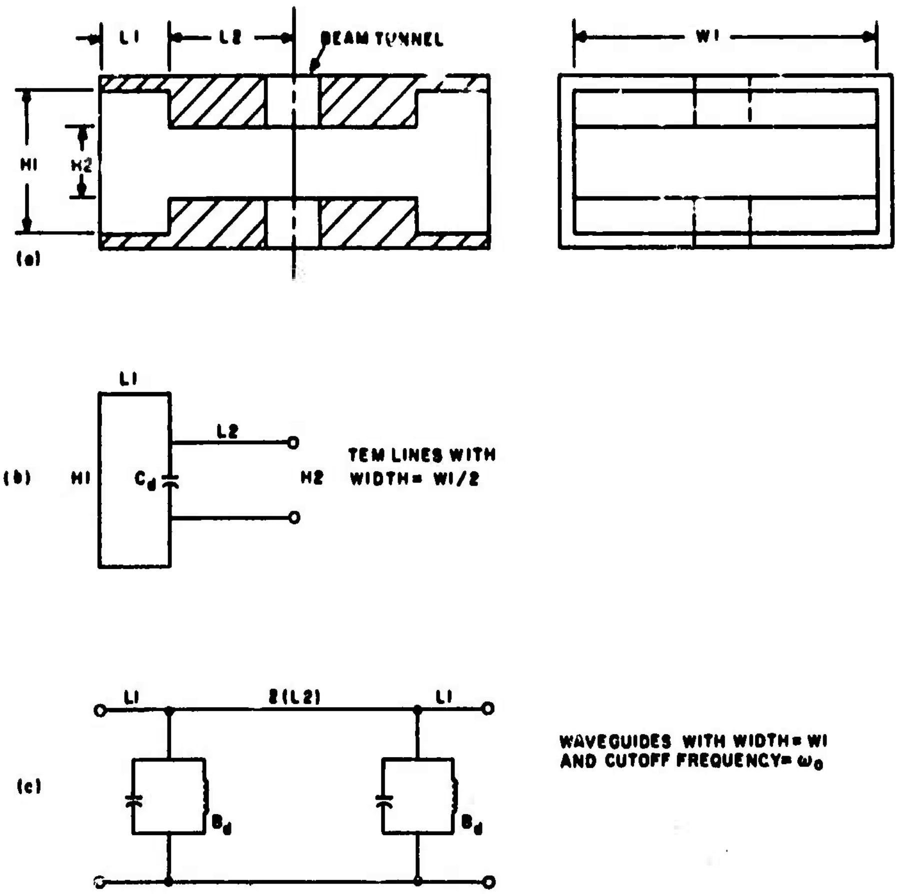

Figure 10 - Physical Layout and Equivalent Circuits for Output Waveguide Sections

The ridged-guide cutoff may be calculated from the resonance of two lengths of TEM line (having widths of W 1/2 plus a discontinuity capacitance, C_d[2], as indicated in Figure 10(b). That is:

$$\omega_r C_d - \frac{W1}{754H1} \operatorname{ctn}\left[\frac{\omega_r L1}{c}\right] + \frac{W1}{754H2} \tan\left[\frac{\omega_r L2}{c}\right] = 0 \qquad (9)$$

where c is the velocity of light. The filter design is simplified by assuming the following approximate relation for C_d:

$$\frac{C_d}{W1} \approx 1.1\left[\frac{H1}{H2}\right] - 1 \quad \text{(picofarads/meter) for } \frac{H1}{H2} < 5 \qquad (10)$$

If ω_o and ω_π (from which ω_r and W1 are determined) plus L1, L2, and one of the heights are specified, the approximation allows direct solution for the other height. If H1 is specified, the resulting equation for H2 is linear, whereas specifying H2 yields a quadratic in H1.

The phase shift and impedance response of the filter may be calculated from the equivalent circuit shown in Figure 10(c). At π mode, this equivalent circuit yields:

$$B_d - \left[\frac{W1}{754H1}\right]\sqrt{1-\left(\frac{\omega_o}{\omega}\right)^2} \operatorname{ctn}\left(\frac{\omega_\pi L_1}{c}\sqrt{1-\frac{\omega_o}{\omega}^2}\right)$$
$$+\left[\frac{W1}{754H2}\right]\sqrt{1-\left(\frac{\omega_o}{\omega}\right)^2} \tan\left(\frac{\omega_\pi L_2}{c}\sqrt{1-\frac{\omega_o}{\omega}^2}\right) = 0 \qquad (11)$$

Because of the relationship between the three frequencies (ω_o, ω_π, and ω_r), the arguments of the tangent and cotangent functions in this equation and the one given previously for the ridged-guide are the same. Multiplying the ridged-guide equation by the radical and subtracting yields:

$$B_d = \omega_r C_d \sqrt{1-\left(\frac{\omega_o}{\omega_\pi}\right)^2} = \omega_\pi C_d \left[1-\left(\frac{\omega_o}{\omega}\right)^2\right] \qquad (12)$$

---

2. J. R. Whinnery and H. W. Jamieson, "Equivalent Circuits for Discontinuities in Transmission Lines", Proc. IRE, Vol. 32, pp. 98-114, Feb. 1944.

Since L1 and L2 may be adjusted to tune ω_π to any frequency without altering the value of C_d, ω_π in the previous equation may be taken as any arbitrary frequency, ω. Thus, the discontinuity susceptance is a parallel resonant circuit with a resonant frequency equal to the guide cutoff frequency and a capacitance equal to the discontinuity capacitance of TEM lines with the same heights and one-half the width.

The phase shift per section may be calculated from the open and short-circuited admittances of a half-section as indicated in Figure 11 (also refer to page 6 of the Quarterly Progress Report No. 1).

$$\beta L = 2 \tan^{-1}\left[\frac{Y_{oc}}{Y_{sc}}\right] = 2 \tan^{-1}\left[\frac{Y'_{oc}}{Y'_{sc}}\right] \qquad (13)$$

The characteristic impedance at the plane of the beam is:

$$Z_o \text{ (beam)} = \frac{1}{\sqrt{Y_{oc}\, Y_{sc}}} \qquad (14)$$

The characteristic impedance at the plane midway between beams is:

$$Z_o \text{ (mid)} = \frac{1}{\sqrt{Y'_{oc}\, Y'_{sc}}} \qquad (15)$$

A BASIC program (THAL 22) for designing and analyzing these filters is given in Appendix B. The required input quantities are f_o, f_π, H1 or H2, L1, and L2. The program computes the other height and the width plus βL, Z_o(beam), and Z_o(mid) across a specified frequency range.

Figure 12 shows the computed phase shift response for a filter of this type and the experimental resonances of a four-section model with and without the beam holes. A capacitively loaded waveguide designed for the same beam-to-beam separation and cutoff frequencies has a computed response that agrees within a phase shift of about one degree at all frequencies.

In order to maintain good coupling to the electron beam, the height (H2) must not exceed 0.170 inch. Furthermore, L2 must exceed 0.100 inch to allow for the 0.100-inch-radius beam hole. As a result, the two-height circuit is most suitable for impedance levels below 700 ohms.

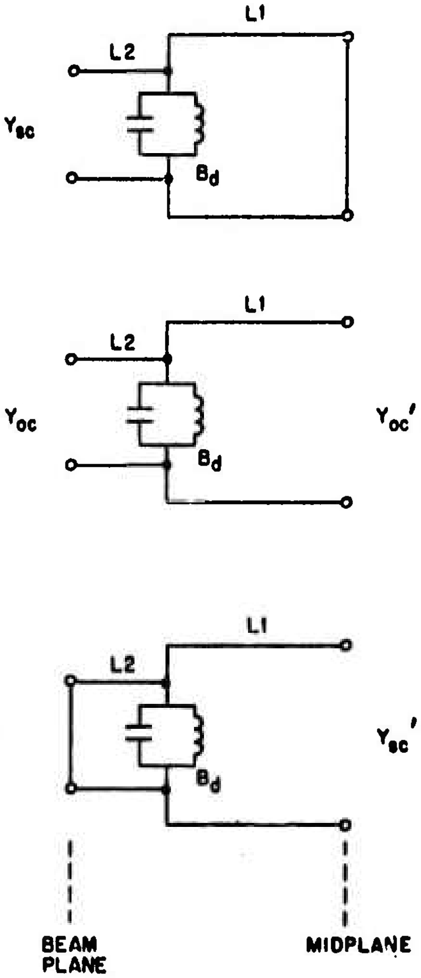

Figure 11 - Equivalent Open- and Short-Circuit Half-Sections

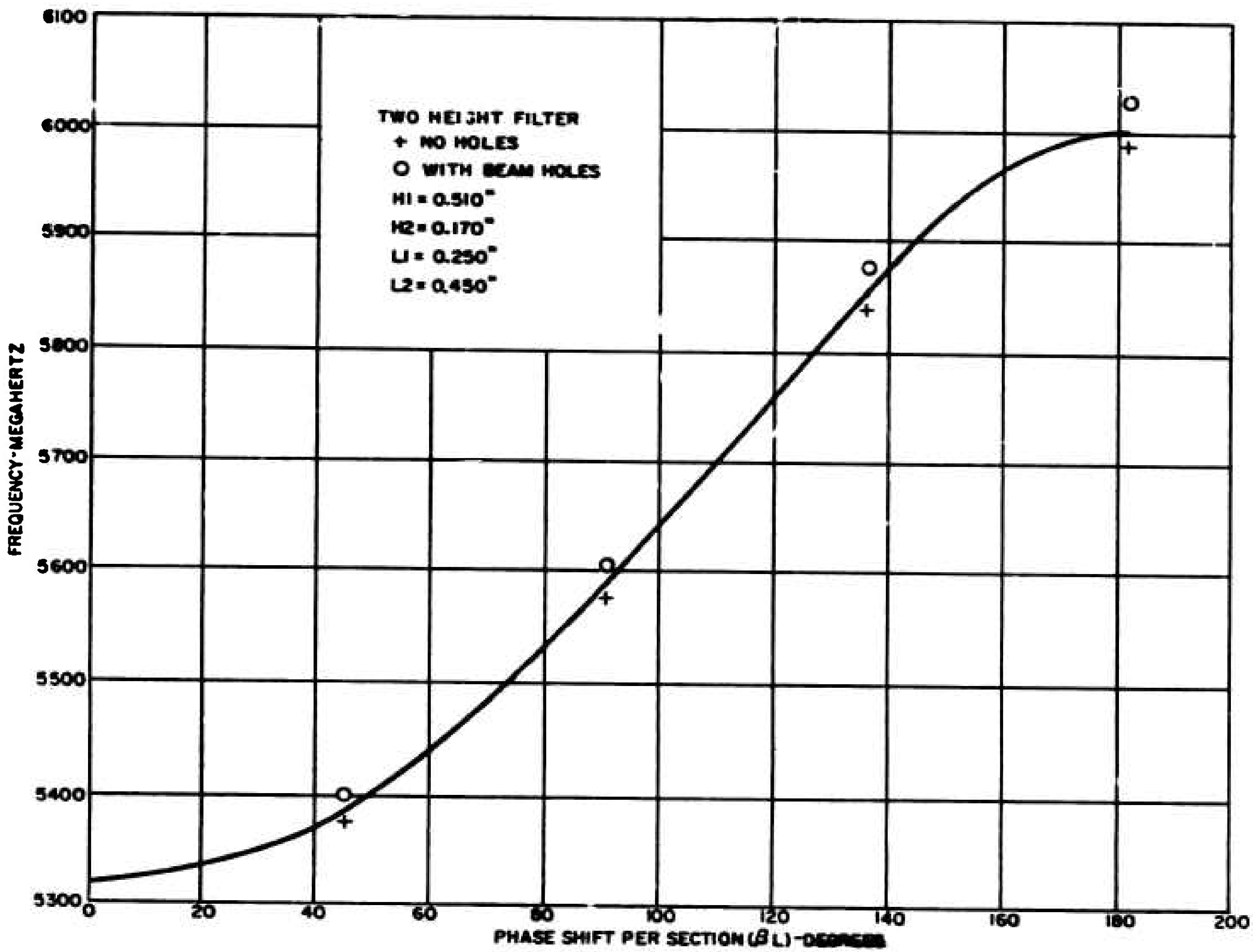

Figure 12 - Frequency-Phase Shift (ω-β) Plot for Output Waveguide (Power Section)

Intermediate-Impedance Circuit

Intermediate values of interaction impedance (i.e. between 700 and 2200 ohms) can be obtained with a hybrid circuit employing the two different height regions defined in Figure 10 plus capacitive tunnel noses. Since this circuit has one more degree of freedom than the two-height filter, it is possible to specify both heights (H1 and H2) as well as both lengths (L1 and L2) and the two cutoff frequencies. The dependent variables are the width and the gap capacitance, C_g. A direct solution is not possible, but an iterative computer solution is convenient.

At π mode, a voltage minimum (short circuit) exists between beams, and a maximum (open circuit) at the beams. Thus, referring to Figure 11 and adding $C_g/2$ at the left side of each circuit, we obtain:

$$j\omega_\pi C_g/2 + Y_{sc}\Big|_{\omega=\omega_\pi} = 0 \tag{16}$$

The zero mode has open circuits at both planes so that:

$$j\omega_o C_g/2 + Y_{oc}\Big|_{\omega=\omega_o} = 0 \tag{17}$$

The admittances, Y_{sc} and Y_{oc}, are not simply related to the width, W1, or the waveguide cutoff frequency, f_c. However, the problem may be linearized by assuming that for small variations in f_c:

$$\Delta Y = \left[\frac{dY}{df_c}\right] \Delta f_c \tag{18}$$

Thus, for an initial estimate of f_c, we have:

$$j\omega_\pi C_g/2 + Y_{sc}\Big|_{\omega=\omega_\pi} + \left[\frac{dY_{sc}}{df_c}\right]_{\omega=\omega_\pi} \Delta f_c = 0 \tag{19}$$

$$j\omega_c C_g/2 + Y_{oc}\Big|_{\omega=\omega_o} + \left[\frac{dY_{oc}}{df_c}\right]_{\omega=\omega_o} \Delta f_c = 0 \tag{20}$$

Solving simultaneously

$$\Delta f_c = \frac{\omega_\pi V_{oc} - \omega_o V_{\pi c}}{\omega_o \left[\frac{dV_{\pi c}}{df_c}\right] - \omega_\pi \left[\frac{dV_{oc}}{df_c}\right]} \tag{21}$$

An improved estimate of f_c is then

$$f_c'' = f_c + \Delta f_c \tag{22}$$

and the procedure is repeated. After the iterative procedure converges on a value for f_c, C_g may be determined directly.

A BASIC program ([illegible]) for designing and analyzing these capacitively loaded, two-height filters is given in Appendix C. The program initially sets f_c halfway between f_o and f_π and then makes seven iterations (giving five or more significant figures). The derivatives are evaluated numerically by making a two-percent change in f_c. The program requires f_o, f_π, H1, H2, L1, and L2 and computes W1 (or f_c) and C_g plus βL, Z_o (beam) and Z_o (mid) across a specified frequency range.

Figure 13 presents the computed phase shift response of a hybrid filter and the experimental resonances of a four-section model. The gap capacitance was set experimentally by varying all four gaps in unison until the 90-degree mode had the correct frequency.

High-Impedance Circuit

The high-impedance circuit used in the build-up region is a special case of the previous circuit in which both heights are the same (i.e., H1 = H2). It may be designed by the same computer program or by the graphical methods described previously in pages [illegible] of Quarterly Progress Report No. 1. Experimental measurements on the high-impedance filter show that the equivalent circuit of a capacitively loaded waveguide predicts somewhat too small a bandwidth. Since the capacitive tunnels have finite dimensions, it appears reasonable to reduce the effective length of the uniform waveguide. The use of an "equivalent" half-section length (L1 + L2) of [illegible]-inch, instead of the actual length of [illegible] inch gives virtually perfect agreement between the measured and computed phase characteristics, if the zero- and π-mode frequencies are set equal to [illegible] and [illegible].

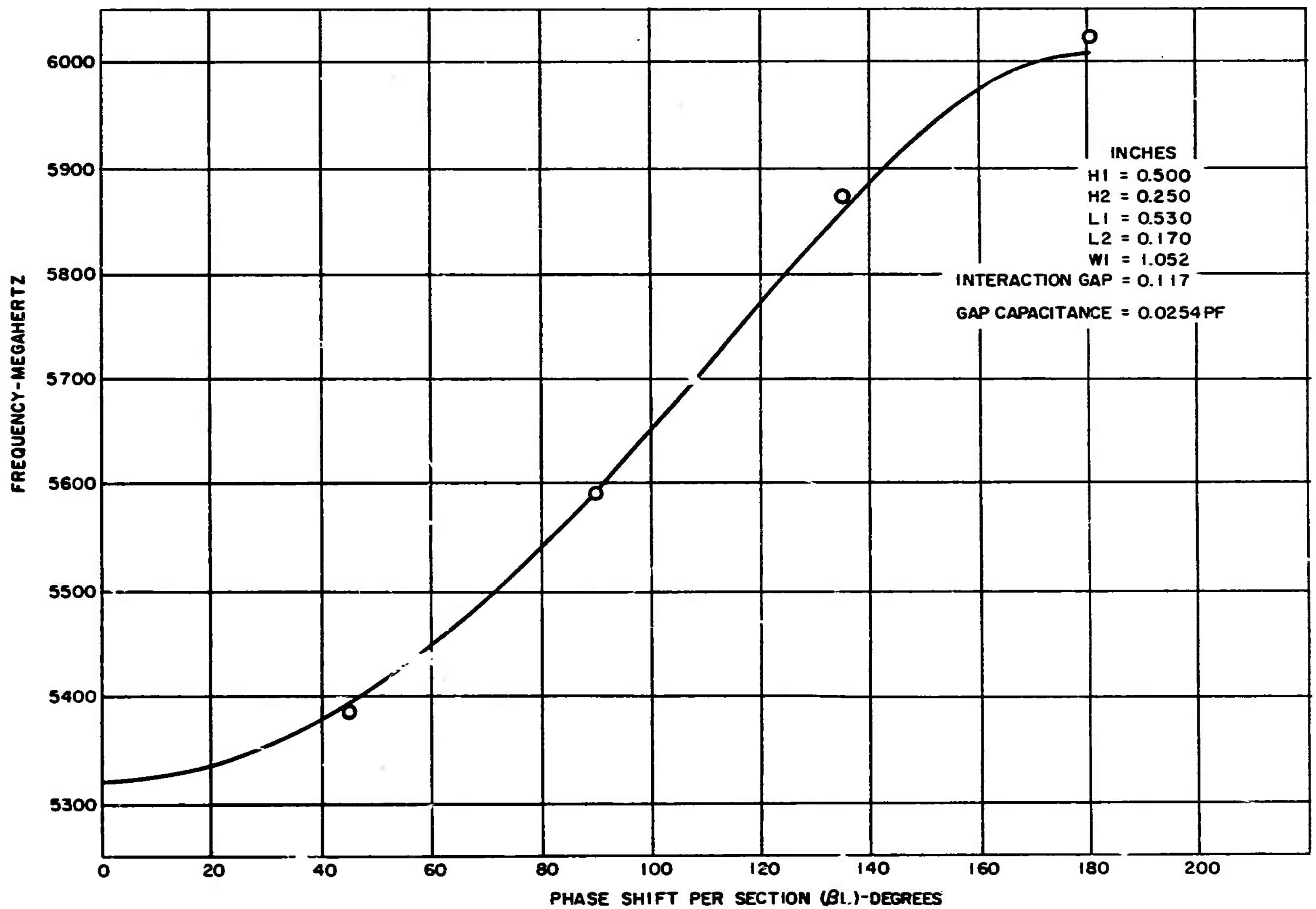

Figure 13 - Frequency-Phase Shift (ω-β) Plot for Output Waveguide (Build-Up Section)

respectively, the required width is 0.983 inch. The resulting phase shift and impedances at the center and edges of the operating band are:

Freq (MH_z)	βL (degrees)	Z_o (beam)	Z_o (mid)
5370	43.8	3802.	1430.
5650	102.6	2260.	535.
5930	152.8	3899.	192.

Design of Tapered Output Circuit

A preliminary design for a tapered output circuit has been accomplished using the circuit forms and computer programs described. Table IV gives the dimensions and mid-band performance of each section. The design of the high-impedance build-up circuit had already been determined by general considerations such as cathode diameter, beam diameter, and beam coupling as described in earlier reports. Although a certain amount of computer cut-and-try was involved, the following general steps were followed in the taper design:

1. Determine the value of Z_o (beam) required for each section from the RF voltage-current characteristics of the beam using the program of Appendix A.

2. Investigate geometries of the two-height circuit that are suitable for the lowest impedance (last) section using the BASIC program of Appendix B. The impedance is essentially directly proportional to H2 and decreases as L2 increases. Check that H1 is reasonable and that the RF electric field intensity at the band edges (where the impedance is highest) is not excessive.

3. Investigate geometries in which H2 equals 0.170 inch (the maximum gap for good electron coupling) and H1 equals 0.500 inch (the height of the uniform circuit), to determine the maximum impedance level and thus the lowest beam position index for which the two-height circuit is suitable. In this case, section 8 is the first of the two-height design.

4. Construct a smooth taper of values of H1 for the two-height sections since abrupt changes in H1 represent an unwanted discontinuity between sections. (Note the progression of H1 in section 8 through 15 of Table IV.) For each of these sections,

Table IV - Preliminary Output Circuit Design

Section Number	Width (in)	H1 (in)	H2 (in)	L1 (in)	L2 (in)	$C_g/2$ (pf)	At 5650 MH_z βL (degrees)	Z_o(beam) (Ohms)	Z_o(mid) (Ohms)
1, 2, 3	0.983	0.500	0.500	0.350	0.350*	0.032	102.6	2262	535
4	1.023	0.500	0.340	0.320	0.380	0.032	103.0	1470	487
5	1.056	0.500	0.255	0.320	0.380	0.027	102.8	1066	450
6	1.080	0.500	0.212	0.290	0.410	0.020	102.8	841	412
7	1.099	0.500	0.182	0.260	0.440	0.0098	102.9	681	375
8	1.114	0.460	0.157	0.274	0.426	0	102.7	581	346
9	1.114	0.430	0.140	0.242	0.458	0	103.0	503	300
10	1.114	0.405	0.126	0.219	0.418	0	103.2	444	265
11	1.114	0.380	0.114	0.204	0.496	0	103.3	397	238
12	1.114	0.355	0.103	0.194	0.506	0	103.4	359	215
13	1.114	0.330	0.094	0.189	0.511	0	103.4	327	196
14	1.114	0.305	0.087	0.187	0.513	0	103.3	300	180
15	1.114	0.287	0.081	0.185	0.515	0	103.3	281	168

* "Equivalent length" of 0.3309 used in calculations

adjust L1 (keeping L1 plus L2 constant) and interpolate to obtain the desired impedance level (if possible). Note that the ratio of Z_0 (beam) to Z_0 (mid) at mid-band stays constant (at 1.65 in this case) within a few percent so that there is a cold mismatch between each section equal to the relative change in Z_0 (beam).

5. Construct a table of values of Z_0 (mid) for the hybrid stages to provide a smooth transition between the build-up sections and the first two-height section (e.g. let Z_0 (mid) vary exponentially in the hybrid sections). (Note the progression of Z_0 (mid) in sections 4 through 7 of Table IV.) Since the hybrid sections have one more degree of freedom than the two-height ones, the ratio between Z_0 (beam) and Z_0 (mid) may be varied.

6. For each hybrid stage, let H1 equal 0.500 inch (the height of the uniform circuit) and vary H2 and L1 to obtain the required values of Z_0 (beam) and Z_0 (mid). Note that, in general terms, changing L1 changes the value of both impedances, whereas varying H2 alters the ratio.

The dimensions given in Table IV have been chosen to yield identical computed cutoff frequencies for all sections. However, there is a slight discrepancy between the calculated and computed frequencies, as illustrated in Figures 12 and 13. These deviations result from neglecting the beam hole in the two-height circuit and the finite dimensions of the capacitive gap in the hybrid circuit. Cold-test models of a few different sections will yield estimates of the shift in cutoff frequencies, and the sections can be redesigned accordingly. For example, Figure 12 shows that the beam holes increase the zero- and π-mode frequencies 23 and 37 MHz, respectively. Thus, the sections which are similar to this model should be redesigned by specifying cutoff frequencies too low by the respective amounts. In the case of section number eight, this redesign changes H2 from 0.157 to 0.159 inch, and the width from 1.114 to 1.118 inch, with the other dimensions unchanged.

The two-height circuit lends itself to an alternate impedance tapering scheme which may be advantageous where a larger transformation ratio or a higher power capability is required. In this technique the beam hole is moved transversely from the center of the guide towards the side wall where the electric field is weaker. Since the electric field distribution is

sinusoidal, the impedance transformation, μ^2, is given (for small holes) by:

$$\mu^2 = \cos^2 \left[\frac{\pi D}{W1}\right] \tag{23}$$

where D is the displacement from guide center. In this type of circuit the hole represents a relatively minor perturbation so that moving it towards the side should have only a small effect on the phase characteristic.

D. CONCLUSIONS

1. The major components of the tube -- cathode, gun structure, input and output waveguides, loaded cavities and collector -- have been built and tested as close to full-power operating conditions as possible.

2. Assembly of these components into a single-beam RF tube is almost complete.

3. Test equipment for the single-beam tube is complete.

4. The magnet for the 15-beam tube is complete.

5. The modulator for the 15-beam tube is in the early stages of construction.

6. The two most difficult theoretical parts of the program -- the beam interaction calculation and the output waveguide impedance taper -- are complete.

7. No insurmountable technical problems are foreseen in the attainment of the objectives of this project.

E. RECOMMENDATIONS AND FUTURE PLANS

1. The immediate objective is the completion and testing of the single-beam tube.

2. Parts for the 15-beam tube which do not depend critically on the single-beam data will be machined.

3. The beam interaction and impedance taper calculations will be re-run using measured values from the single-beam tests, and drawings for the cavities and output waveguide will be revised.

4. When testing of the single-beam tube is complete, the test engineers will work on construction of the 150-KW modulator.

Appendix A - Computer Program (THAL21) for Calculating Impedance Taper

```
100 DATA 19.4,16.37,53550,2260
110   REM IMPEDANCE TAPER CALCULATION
120 READ I0,I1,V1,Z0
130   REM AMPS, VOLTS, AND OHMS
140 PRINT "INDUCED I","INDUCED I","V MAX","Z(0)"
150 PRINT "AT V=0"    ,"AT V=V MAX"," ",  "UNIFORM"
160 PRINT I0,I1,V1,Z0
170 PRINT "BEAM NO.","Z(N)","Z(N)/Z(0)","I FWD","V(N)"
180 LET S=SQR(Z0)
190 LET I=0
200   REM CALC VOLTAGE (V) AND FORWARD CURRENT (I) IN BUILD-UP
210 FOR M=1 TO 15 STEP 1
220 LET V=Z0*(I+I0/2)/(1-.5*Z0*(I1-I0)/V1)
230   REM IF VOLTAGE EXCEEDS OPTIMUM CALCULATE REDUCED Z
240 IF V>V1 THEN 290
250 LET I=I+(I0+(I1-I0)*V/V1)/2
260 PRINT M,Z0," 1",I,V
270 NEXT M
280   REM CALC I AND LINE IMPEDANCE AT EACH POWER BEAM
290 FOR N=M TO 15 STEP 1
300 LET A=I1/2
310 LET B=I*S
320 LET C=-V1
330 LET R9=SQR(B*B-4*A*C)
340 LET S1=(-B+R9)/(2*A)
350 LET Z=S1*S1
360 LET I=I*S/S1+I1/2
370 PRINT N,Z,Z/Z0,I
380 LET S=S1
390 NEXT N
400 LET P=.5E-6*Z*I*I
410 LET B=2*V1/I1/Z0
420 PRINT "PWR OUT (MW)","EQUIV Z/.5Z(0)"
430 PRINT P,B
440 PRINT
450 GOTO 120
460 END
```

Appendix B - Computer Program (THAL 22) for Designing Output Waveguide

```
100 DATA 5300,5990,0,.08,.15,.55
101 DATA 5300,5990,.318099,0,.15,.55
110   REM DESIGN OF TWO-HEIGHT WAVEGUIDE FILTER
120 READ F0,F9,H1,H2,L1,L2
130   REM MHZ AND INCHES
140   REM H1 IS UNKNOWN UNLESS H2=0 IN WHICH CASE H2 IS UNKNOWN
150 LET W1=5901.4/F0
160 PRINT "F(0)","F(P1)","LENGTH(1)","LENGTH(2)","WIDTH"
170 PRINT F0,F9,L1,L2,W1
180   REM CALCULATE REQUIRED F(CUTOFF)=F3 OF TRANSVERSE RIDGED GUIDE
190 LET F3=F9*SQR(1-(F0/F9)↑2)
200   REM CALCULATE TAN(BL) FOR L1 AND L2 AT F3
210 LET W=6.28318E6*F3
220 LET V=1.18029E10
230 LET T1=TAN(W*L1/V)
240 LET T2=TAN(W*L2/V)
250   REM SOLVE EQUATION FOR HEIGHT H1 (QUADRATIC) OR H2 (LINEAR)
260 LET A=10.5334E-12*W
270 IF H2=0 THEN 330
280 LET B=-H2+T2/A
290 LET C=-H2/T1/A
300 LET R9=SQR(B*B-4*C)
310 LET H1=(-B+R9)/2
320 GO TO 340
330 LET H2=(H1*H1*A+T2*H1)/(H1*A+1/T1)
340 LET Z1=754*H1/W1
350 LET Z2=754*H2/W1
360 LET F1=F0
370 LET C=82.445*(H1/H2-1)/F1
380 PRINT "HEIGHT(1)","HEIGHT(2)","C(DIS)","F(CUTOFF)"
390 PRINT H1,H2,C,F1
400 PRINT "FREQ","BETA L","Z(0) AT BEAM","Z(0) MID"
410 FOR F=5370 TO 5930 STEP 140
420   REM CALCULATE WAVEGUIDE PARAMETERS
430 LET R0=1-(F1/F)↑2
440 LET R1=SQR(ABS(R0))
450 LET B=5.3235E-4*F*R1
460   REM RADIANS PER INCH
470 LET S=-1
480 LET T1=TAN(B*L1)
490 LET T2=TAN(B*L2)
500   REM CALCULATE X'S OF LINE 1 OPEN (X1) AND SHORTED (Y1)
510 LET X1=Z1*T1/R1
520 LET Y1=S*Z1/T1/R1
530   REM ADD DISCONTINUITY SUSCEPTANCE (B9)
540 LET B9=6.28318E-6*F*C
550 LET B9=B9*R0
560 LET X1=X1/(1-X1*B9)
570 LET Y1=Y1/(1-Y1*B9)
580   REM TRANSFORM X'S ALONG LINE 2
590 LET Z3=Z2/R1
600 LET X4=Z3*(X1+Z3*T2)/(Z3+S*X1*T2)
610 LET Y4=Z3*(Y1+Z3*T2)/(Z3+S*Y1*T2)
620   REM CHECK WHETHER FILTER PROPAGATES
630 IF (-X4/Y4) >0 THEN 670
640 PRINT F
650 GOTO 790
660   REM CALCULATE BETA L AND Z(0)'S AT BEAM AND MID PLANES
670 LET 02=57.2958*ATN(SQR(-X4/Y4))
680 LET D2=2*02
690 LET Z=SQR(-X4*Y4)
700 LET Z4=Z1/R1
710 LET X2=Z3*T2
720 LET Y2=Z3/(S*T2)
730 LET X2=X2/(1-X2*B9)
740 LET Y2=Y2/(1-Y2*B9)
750 LET X5=Z4*(X2+Z4*T1)/(Z4+S*X2*T1)
760 LET Y5=Z4*(Y2+Z4*T1)/(Z4+S*Y2*T1)
770 LET Y=SQR(-X5*Y5)
780 PRINT F,02,Z,Y
790 NEXT F
800 PRINT
810 GO TO 120
820 END
```

Appendix C - Computer Program (THAL 23) for Designing Capacitively Loaded Waveguide

```
100 DATA 5300,5990,.5,.34,.32,.38
110   REM C-LOADED, TWO-STEP WAVEGUIDE DESIGN AND CALCULATION
120 READ F0,F9,H1,H2,L1,L2
130   REM MHZ AND INCHES
140 PRINT "F(ZERO)","F(PI)"
150 PRINT F0,F9
160 PRINT "HEIGHT(1)","HEIGHT(2)","LENGTH(1)","LENGTH(2)"
170 PRINT H1,H2,L1,L2
180 LET F2=(F0+F9)/2
190   REM START OF ITERATIVE LOOP
200 FOR N=1 TO 7 STEP 1
210   REM CALCULATE B(ZERO)=B1
220 LET F=F0
230 LET F1=F2
240 GOSUB 550
250 LET B8=-R1*Y1*T1*S
260 GOSUB 750
270 LET B1=B8
280   REM INCREMENT F(CUTOFF) AND RECALCULATE B(ZERO)=B3
290 LET F1=1.02*F2
300 GOSUB 550
310 LET B8=-R1*Y1*T1*S
320 GOSUB 750
330 LET B3=B8
340   REM CALCULATE B(PI)=B2
350 LET F=F9
360 LET F1=F2
370 GOSUB 550
380 LET B8=-R1*Y1/T1
390 GOSUB 750
400 LET B2=B8
410   REM INCREMENT F(CUTOFF) AND RECALCULATE B(PI)=B4
420 LET F1=1.02*F2
430 GOSUB 550
440 LET B8=-R1*Y1/T1
450 GOSUB 750
460 LET B4=B8
470   REM CALCULATE DB/DF(C) AT ZERO AND PI MODES
480 LET D0=(B3-B1)/(.02*F2)
490 LET D9=(B4-B2)/(.02*F2)
500   REM CALCULATE NEW ESTIMATE OF F(CUTOFF)
510 LET F2=F2+(F9*B1-F0*B2)/(F0*D9-F9*D0)
520 NEXT N
530 GOTO 780
540   REM SUBROUTINE TO CALCULATE WAVEGUIDE PARAMETERS
550 LET R0=1-(F1/F)↑2
560 LET R1=SQR(ABS(R0))
570 LET B=5.3235E-4*F*R1
580   REM RADIANS/INCH
590 LET C=82.445*(H1/H2-1)/F1
600 LET W1=5901.4/F1
610 LET Y1=W1/754/H1
620 LET Y2=W1/754/H2
630 IF F>F1 THEN 700
640 LET S=1
650 LET E1=EXP(2*B*L1)
660 LET E2=EXP(2*B*L2)
670 LET T1=(E1-1)/(E1+1)
680 LET T2=(E2-1)/(E2+1)
690 GOTO 730
700 LET S=-1
710 LET T1=TAN(B*L1)
720 LET T2=TAN(B*L2)
730 RETURN
```

Appendix C (Cont.)

```
740   REM SUBROUTINE TO ADD DISC B AND TRANSFORM B ALONG LINE 2
750 LET B8=B8+6.28318E-6*F*C*R0
760 LET B8=R1*Y2*(B8-S*Y2*R1*T2)/(Y2*R1-B8*T2)
770 RETURN
780 LET C1=-B1/(6.28318E-6*F0)
790 LET W1=5901.4/F2
800 PRINT "C(GAP)/2","WIDTH","F(CUTOFF)"
810 PRINT C1,W1,F2,.106*(H2-.17)
820 LET Z1=754*H1/W1
830 LET Z2=754*H2/W1
840 LET F1=5901.4/W1
850 PRINT "FREQ","BETA L","Z(0) AT BEAM","Z(0) MID"
860 FOR F=5650 TO 5651 STEP 100
870 GOSUB 550
880   REM CALCULATE X'S OF LINE 1 OPEN (X1) AND SHORTED (Y1)
890 LET X1=Z1*T1/R1
900 LET Y1=S*Z1/T1/R1
910   REM ADD DISCONTINUITY SUSCEPTANCE (B9)
920 LET B8=6.28318E-6*F*C1
930 LET B9=6.28318E-6*F*C
940 LET B9=B9*R0
950 LET X1=X1/(1-X1*B9)
960 LET Y1=Y1/(1-Y1*B9)
970   REM TRANSFORM X'S ALONG LINE 2 AND ADD GAP SUSCEPTANCE (B8)
980 LET Z3=Z2/R1
990 LET X4=Z3*(X1+Z3*T2)/(Z3+S*X1*T2)
1000 LET X4=X4/(1-X4*B8)
1010 LET Y4=Z3*(Y1+Z3*T2)/(Z3+S*Y1*T2)
1020 LET Y4=Y4/(1-Y4*B8)
1030   REM CHECK WHETHER FILTER PROPAGATES
1040 IF (-X4/Y4) >0 THEN 1080
1050 PRINT F
1060 GOTO 1200
1070   REM CALCULATE BETA L AND Z(0)'S AT BEAM AND MID PLANES
1080 LET D2=57.2958*ATN(SQR(-X4/Y4))
1090 LET D2=2*D2
1100 LET Z=SQR(-X4*Y4)
1110 LET Z4=Z1/R1
1120 LET X2=Z3*T2
1130 LET Y2=Z3*(-1+B8*Z3*T2)/(Z3*B8-S*T2)
1140 LET X2=X2/(1-X2*B9)
1150 LET Y2=Y2/(1-Y2*B9)
1160 LET X5=Z4*(X2+Z4*T1)/(Z4+S*X2*T1)
1170 LET Y5=Z4*(Y2+Z4*T1)/(Z4+S*Y2*T1)
1180 LET Y=SQR(-X5*Y5)
1190 PRINT F,D2,Z,Y,Z/Y
1200 NEXT F
1210 PRINT
1220 GOTO 120
1230 END
```

Security Classification

DOCUMENT CONTROL DATA - R&D

(Security classification of title, body of abstract and indexing annotation must be entered when the overall report is classified)

1. ORIGINATING ACTIVITY (Corporate author) General Electric Company Schenectady, New York	2a. REPORT SECURITY CLASSIFICATION UNCLASSIFIED 2b. GROUP N/A

3. REPORT TITLE

HIGH-POWER HYBRID MULTIPLE-BEAM KLYSTRON FOR PHASED ARRAYS

4. DESCRIPTIVE NOTES (Type of report and inclusive dates)

Sixth Quarterly Progress Report - 15 December to 15 March 1967

5. AUTHOR(S) (Last name, first name, initial)

Branch, G. M. - Neugebauer, W. - Thal, H. L. - Vaughan, J. R. M.

6. REPORT DATE	7a. TOTAL NO. OF PAGES	7b. NO. OF REFS
June 1967	37	

8a. CONTRACT OR GRANT NO. DA 28-043 AMC-01666(E) b. PROJECT NO. 7900.21.223.12.00.50.410-6 c. d.	9a. ORIGINATOR'S REPORT NUMBER(S) 9b. OTHER REPORT NO(S) (Any other numbers that may be assigned this report) ECOM-01666-6

10. AVAILABILITY/LIMITATION NOTICES This document is subject to special export controls and each transmittal to foreign governments or foreign nationals may be made only with prior approval of CG, USAECOM ATTN: AMSEL-KL-TM, Fort Monmouth, New Jersey 07703

11. SUPPLEMENTARY NOTES ARPA ARPA ORDER NO. 345 AMENDMENT NO. 2	12. SPONSORING MILITARY ACTIVITY U.S. Army Electronics Command Fort Monmouth, N.J. AMSEL-KL-TM

13. ABSTRACT

The purpose of this contract is the development of a high-power broadband amplifier using the principles of a traveling-wave multiple-beam klystron. The method being followed is to (a) design the beam and the interaction impedances by a computer study, (b) build a single-beam prototype for checking the calculations and obtaining final data, and (c) construct a full-power 15-beam tube.

At this point in the program, the beam and interaction designs have been completed, and fabrication of the single-beam prototype tube is almost complete. Test equipment for the single-beam tube has been set up, the modulator for the 15-beam tube has been designed, and major components are being received. The electromagnet for the 15-beam tube is in place, and the single-beam tube is to be tested in various positions in it.

Conclusions: All basic elements for the single-beam prototype have been designed, fabricated, and tested. The assembly is almost complete, and processing and testing of this tube can now proceed. No major problems are foreseen.

DD FORM 1 JAN 64 1473

Security Classification

14. KEY WORDS	LINK A		LINK B		LINK C	
	ROLE	WT	ROLE	WT	ROLE	WT
Multiple-Beam Klystron						
Broadband Microwave Amplifier						
Periodically-Loaded Waveguide						
Microwave Circuit Analysis						
Traveling Wave Klystron						
C-Band Amplifier						
Phased Arrays						

INSTRUCTIONS

1. ORIGINATING ACTIVITY: Enter the name and address of the contractor, subcontractor, grantee, Department of Defense activity or other organization *(corporate author)* issuing the report.

2a. REPORT SECURITY CLASSIFICATION: Enter the overall security classification of the report. Indicate whether "Restricted Data" is included. Marking is to be in accordance with appropriate security regulations.

2b. GROUP: Automatic downgrading is specified in DoD Directive 5200.10 and Armed Forces Industrial Manual. Enter the group number. Also, when applicable, show that optional markings have been used for Group 3 and Group 4 as authorized.

3. REPORT TITLE: Enter the complete report title in all capital letters. Titles in all cases should be unclassified. If a meaningful title cannot be selected without classification, show title classification in all capitals in parenthesis immediately following the title.

4. DESCRIPTIVE NOTES: If appropriate, enter the type of report, e.g., interim, progress, summary, annual, or final. Give the inclusive dates when a specific reporting period is covered.

5. AUTHOR(S): Enter the name(s) of author(s) as shown on or in the report. Enter last name, first name, middle initial. If military, show rank and branch of service. The name of the principal author is an absolute minimum requirement.

6. REPORT DATE: Enter the date of the report as day, month, year; or month, year. If more than one date appears on the report, use date of publication.

7a. TOTAL NUMBER OF PAGES: The total page count should follow normal pagination procedures, i.e., enter the number of pages containing information.

7b. NUMBER OF REFERENCES: Enter the total number of references cited in the report.

8a. CONTRACT OR GRANT NUMBER: If appropriate, enter the applicable number of the contract or grant under which the report was written.

8b, 8c, & 8d. PROJECT NUMBER: Enter the appropriate military department identification, such as project number, subproject number, system numbers, task number, etc.

9a. ORIGINATOR'S REPORT NUMBER(S): Enter the official report number by which the document will be identified and controlled by the originating activity. This number must be unique to this report.

9b. OTHER REPORT NUMBER(S): If the report has been assigned any other report numbers *(either by the originator or by the sponsor)*, also enter this number(s).

10. AVAILABILITY/LIMITATION NOTICES: Enter any limitations on further dissemination of the report, other than those imposed by security classification, using standard statements such as:

(1) "Qualified requesters may obtain copies of this report from DDC."

(2) "Foreign announcement and dissemination of this report by DDC is not authorized."

(3) "U. S. Government agencies may obtain copies of this report directly from DDC. Other qualified DDC users shall request through

____."

(4) "U. S. military agencies may obtain copies of this report directly from DDC. Other qualified users shall request through

____."

(5) "All distribution of this report is controlled. Qualified DDC users shall request through

____."

If the report has been furnished to the Office of Technical Services, Department of Commerce, for sale to the public, indicate this fact and enter the price, if known.

11. SUPPLEMENTARY NOTES: Use for additional explanatory notes.

12. SPONSORING MILITARY ACTIVITY: Enter the name of the departmental project office or laboratory sponsoring *(paying for)* the research and development. Include address.

13. ABSTRACT: Enter an abstract giving a brief and factual summary of the document indicative of the report, even though it may also appear elsewhere in the body of the technical report. If additional space is required, a continuation sheet shall be attached.

It is highly desirable that the abstract of classified reports be unclassified. Each paragraph of the abstract shall end with an indication of the military security classification of the information in the paragraph, represented as *(TS)*, *(S)*, *(C)*, or *(U)*.

There is no limitation on the length of the abstract. However, the suggested length is from 150 to 225 words.

14. KEY WORDS: Key words are technically meaningful terms or short phrases that characterize a report and may be used as index entries for cataloging the report. Key words must be selected so that no security classification is required. Identifiers, such as equipment model designation, trade name, military project code name, geographic location, may be used as key words but will be followed by an indication of technical context. The assignment of links, rules, and weights is optional.